

Strongly interactive 0D/2D hetero-structure of $Zn_xCd_{1-x}S$ nano-particle decorated phosphorene nano-sheet for enhanced visible-light photocatalytic H_2 production

*Jingrun Ran^a, Xiuli Wang^b, Bicheng Zhu^c and Shi-Zhang Qiao^{*a}*

^aSchool of Chemical Engineering, The University of Adelaide, Adelaide, SA 5005, Australia

^bState Key Laboratory of Catalysis, Dalian Institute of Chemical Physics,
Chinese Academy of Sciences, Dalian National Laboratory for Clean Energy, Dalian 116023, P. R.
China

^cState Key Laboratory of Advanced Technology for Materials
Synthesis and Processing, Wuhan University of Technology, 122

Luoshi Road, Wuhan 430070, P. R. China

E-mail: s.qiao@adelaide.edu.au

I. Computation section

Computation details

The density functional theory (DFT) calculations were carried out by using the Vienna *ab initio* simulation package (VASP). The exchange-correlation interaction was described by generalized gradient approximation (GGA) with the Perdew-Burke-Ernzerhof (PBE) functional. The energy cutoff and Monkhorst-Pack k-point mesh were set to as 350 eV and $8 \times 8 \times 1$, respectively. During the geometry optimization, the convergence tolerance was set as 1.0×10^{-4} eV for energy and 0.03 eV/Å for force. For the construction of surface models, a vacuum of 20 Å was used to eliminate interactions between periodic images. The DFT-D2 method of Grimme was employed to treat the van der Waals (vdW) interaction. The work function is defined as $\Phi = E_V - E_F$, where E_V and E_F are the electrostatic potentials of the vacuum and Fermi levels, respectively.

To simulate $\text{Zn}_{0.8}\text{Cd}_{0.2}\text{S}$ surface configuration, four possible surface models containing four Zn atom layers, one Cd atom layer and five S atom layers were constructed. In detail, the inner Cd atoms could be placed at the second to the fifth metal atom layer. To determine the most stable and preferential position of Cd atom layer, adhesive energy (E_{ad}) of the four $\text{Zn}_{0.8}\text{Cd}_{0.2}\text{S}/\text{P}$ systems was calculated using $E_{\text{ad}} = E(\text{Zn}_{0.8}\text{Cd}_{0.2}\text{S}/\text{P}) - E(\text{Zn}_{0.8}\text{Cd}_{0.2}\text{S}) - E(\text{P})$, where $E(\text{Zn}_{0.8}\text{Cd}_{0.2}\text{S}/\text{P})$, $E(\text{Zn}_{0.8}\text{Cd}_{0.2}\text{S})$ and $E(\text{P})$ were the energy of $\text{Zn}_{0.8}\text{Cd}_{0.2}\text{S}/\text{P}$ system, fresh $\text{Zn}_{0.8}\text{Cd}_{0.2}\text{S}$ surface and P monolayer. The result was that the E_{ad} for the $\text{Zn}_{0.8}\text{Cd}_{0.2}\text{S}/\text{P}$ systems with Cd atoms placing at the second, fourth and fifth layer was -4.37 eV, -4.35 eV and -4.31 eV, respectively. The $\text{Zn}_{0.8}\text{Cd}_{0.2}\text{S}/\text{P}$ system with Cd atoms placing at the third layer was excluded because its geometry optimization failed. As concluded, the most negative E_{ad} was obtained when the Cd atoms were placed at the second metal atom layer. Therefore, the subsequent research on the electronic property of $\text{Zn}_{0.8}\text{Cd}_{0.2}\text{S}/\text{P}$ composite was performed on the $\text{Zn}_{0.8}\text{Cd}_{0.2}\text{S}/\text{P}$ system with Cd atoms placing at the second metal atom layer.

II. Experimental section

Materials synthesis

The bulk BP crystals was purchased from Smart elements and conserved in a dark glovebox filled with Argon gas. The absolute ethanol ($\geq 99.5\%$, anhydrous) was purchased from Sigma-Aldrich. All the reagents were analytic grade and used without further purification. A liquid-phase exfoliation method was employed to fabricate FLP using an ultrasonic probe followed by ice-bath sonication of bulk BP crystals in absolute ethanol. In detail, 35 mg bulk BP was ground and added into ethanol, followed by ultra-sonication for 180 min. The ultrasonic probe was on for 2 s and off for 4 s. Afterwards, the obtained dispersion was further ultra-sonicated for 300 min at a lower power. An ice bath was applied to keep the temperature of the dispersion below 25 °C during the ultra-sonication process. Then the supernatant was collected after the dispersion centrifuged at 16000 RPM for 15 min. The supernatant were used as FLP ethanol solution. The experiments were carried out in the glove box filled with Argon gas except that the ultra-sonication and centrifugation processes. A precipitation-hydrothermal method was applied to prepare ZCS NP. In detail, 200 mg $\text{Cd}(\text{Ac})_2 \cdot 2\text{H}_2\text{O}$ and 410 mg $\text{Zn}(\text{Ac})_2 \cdot 2\text{H}_2\text{O}$ was added into 22.8 ml deionized water followed by stirring for 60 min. Afterwards, 6 ml of 0.9 M Na_2S aqueous solution was added dropwise into the above solution, followed by stirring for 120 min. At last, the suspension was transferred into a 60 ml Teflon-lined autoclave and kept at 180 °C for 12 hours. The final products were washed by deionized water and ethanol for two times, respectively, and dried at 60 °C for 10 hours. FLP modified ZCS NP was fabricated by mechanically mixing the as-prepared ZCS NP with FLP ethanol solution in a mortar inside a glovebox filled with Argon. In detail, 20 mg of ZCS NP was added into the mortar, followed by adding a certain amount of FLP ethanol solution. Afterwards, the suspension was mechanically ground for 15 min inside the glovebox. After the natural evaporation of ethanol, the remained solid was ground again into fine powders as the final products. The nominal weight ratios of FLP to ZCS were 0.5, 2.0, 6.0 and 9.0 wt%, and the resulting samples were labelled as P0.5, P2, P6 and P9, respectively. 2Pt-ZCS was synthesized by *in-situ* photo-deposition of 2.0 wt% Pt on the as-prepared ZCS NP using H_2PtCl_6 aqueous solution.

Characterisations of physico-chemical properties

A powder X-ray diffractometer (Miniflex, Rigaku) was applied to acquire the XRD patterns at 40 kV and 15 mA using Cu K α radiation. NT-MDT Ntegra Solaris instrument was utilized to obtain AFM image. Raman spectra were acquired on an iHR550 Raman microscope (HORIBA scientific), equipped with a charge-coupled device (CCD) detector and a confocal microscope. JEM-2100F electron microscope (JEOL, Japan) was operated to obtain the TEM and HRTEM images, and EDX spectra. A VG ESCALAB 210 XPS spectrometer system with Mg K α source was applied to conduct XPS measurement. All the binding energies were referenced to the C1s peak at 284.8 eV of the surface adventitious carbon. The synchrotron-based NEXAFS measurements were conducted in an ultrahigh vacuum chamber ($\sim 10^{-10}$ mbar) of the undulator soft X-ray spectroscopy beamline at the Australian Synchrotron. The samples were dispersed in ethanol and then deposited and dried on Au plates. The raw NEXAFS data were normalized to the photoelectron current of the photon beam, measured on an Au grid. A UV-Vis spectrophotometer (UV2600, Shimadzu, Japan) was employed to obtain the UV-visible diffuse reflectance spectra. A RF-5301PC spectrofluorophotometer (Shimadzu, Japan) was used to acquire the steady-state photoluminescence (PL) spectra at room temperature. Transient-state PL decay curves were obtained on a FLS920 fluorescence lifetime spectrophotometer (Edinburgh Instruments, UK). The BET specific surface area and the pore volume of the samples were acquired on a Micromeritics ASAP 2020 N₂ adsorption instrument (USA).

Photocatalytic H₂ production experiment

The photocatalytic H₂ production experiments were conducted in a 100 ml Pyrex flask sealed with silicone rubber septa under room temperature and atmospheric pressure. A 300 W Xenon arc lamp equipped with a UV-cutoff filter ($\lambda \geq 420$ nm) was utilized as the light source to trigger the photocatalytic reaction. The focused intensity on the flask was about 80 mW cm⁻². In a typical photocatalytic experiment, 20 mg photocatalyst was dispersed under continuous stirring in 80 ml mixed aqueous solution of 20 ml lactic acid (88 vol.%) and 60 ml deionized water. Then Argon gas was purged into the dispersion of photocatalyst for 30 min to remove the air prior to

irradiation and ensure the reactor under anaerobic conditions. 0.2 ml gas was sampled intermittently through the septum, and the produced H₂ was tested by gas chromatograph (Clarus 480, Perkin Elmer, USA, thermal conductivity detector (TCD) with Argon as a carrier gas and 5 Å molecular sieve column). Under the identical photocatalytic reaction conditions, the apparent quantum efficiency (QE) was measured. Four low-power 420 nm light-emitting diodes (LEDs) (3 W, Shenzhen LAMPLIC Science Co Ltd. China) were utilized as the light source to drive the photocatalytic reactions. The focused intensity for every 420 nm LED was about 6 mW cm⁻². The QE was determined according to the following equation (1):

$$\begin{aligned} \text{QE}[\%] &= \frac{\text{number of reacted electrons}}{\text{number of incident photons}} \times 100 \\ &= \frac{\text{number of evolved H}_2 \text{ molecules} \times 2}{\text{number of incident photons}} \times 100 \end{aligned} \quad (1)$$

Electrochemical and photoelectrochemical tests

The transient photocurrent (TPC) response measurement was conducted on an electrochemical analyser (CHI760D instruments) in 0.2 M Na₂S and 0.04 M Na₂SO₃ aqueous solution in a standard three-electrode system, using the as-synthesized samples as the working electrode, Ag/AgCl (saturated KCl) as a reference electrode, and a Pt wire as the counter electrode. The light source was a 300 W Xenon light with a UV-cutoff filter ($\lambda \geq 420$ nm). The working electrodes were synthesized as follows: 100 mg sample, 30 mg polyethylene glycol (PEG; molecular weight: 20000) and 0.5 ml ethanol were ground together to make a slurry. After that, a doctor blade method was applied to coat the slurry onto a 2 cm × 1.5 cm FTO glass electrode. The obtained electrode was dried and calcined at 350 °C for 30 min under flowing N₂. The film thickness of all the working electrodes were kept at about 10-11 μm.

III. Supplementary Results

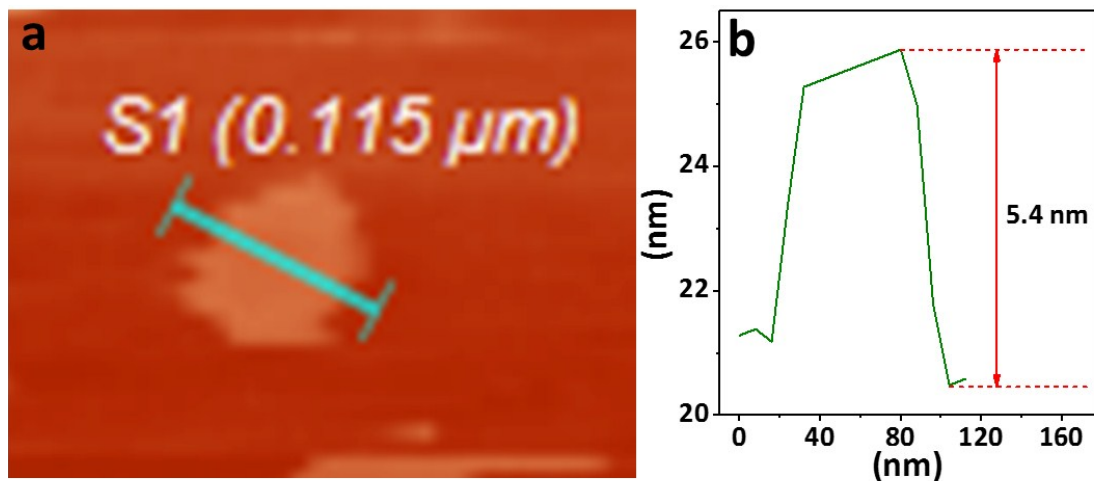


Fig. S1. Typical (a) AFM image of few-layer phosphorene (FLP) and (b) the measured thickness of FLP in (a).

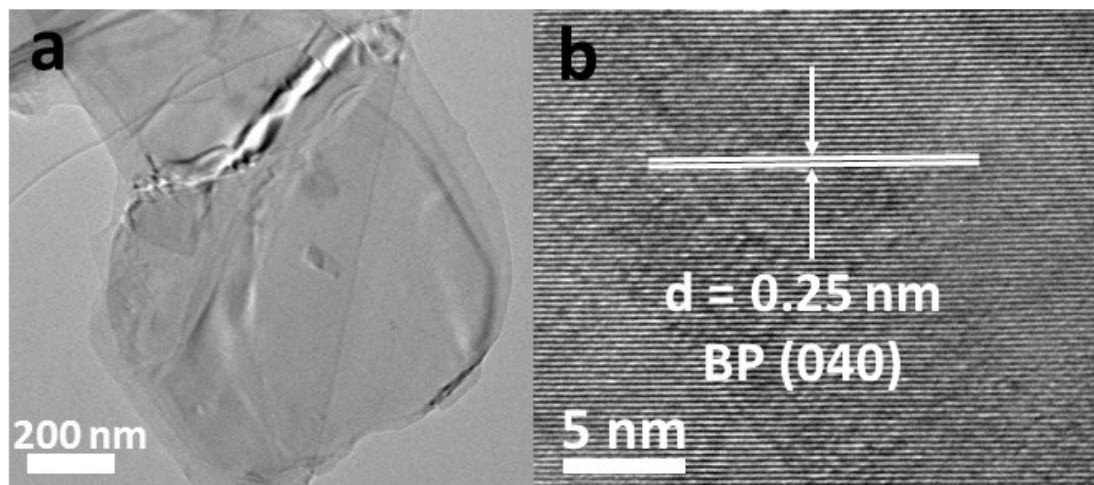


Fig. S2. (a) A typical TEM image and (b) HRTEM image of FLP.

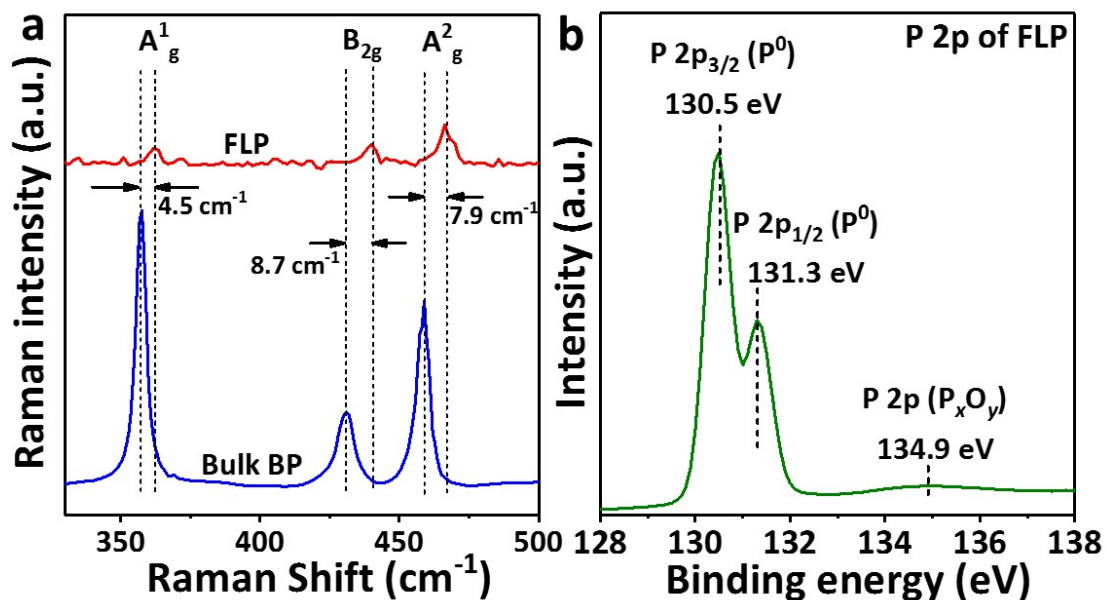


Fig. S3. (a) Raman spectra of bulk black phosphorous (BP) and FLP and (b) high-resolution X-ray photoelectron spectroscopy (XPS) spectrum of P 2p for FLP.

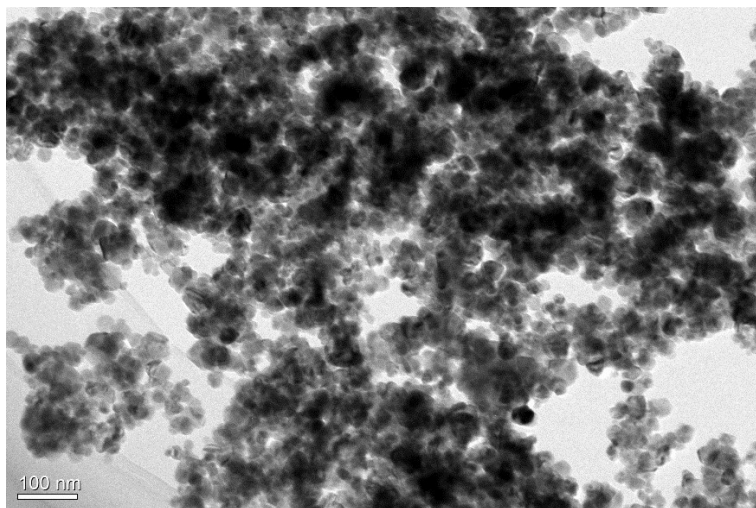


Fig. S4. TEM image of P0.

The coupling of FLP NS with ZCS NPs in P2 (Fig. 1a) improved the dispersion of ZCS NPs compared to ZCS NPs alone (Fig. S4). However, the small size, high surface energy and lack of capping agent of ZCS NPs unavoidably arouse their aggregation to some extent on the surface of FLP NS (Fig. 1a), thus decreasing the exposed surface area and active sites of ZCS NPs in P2. This aggregation will also suppress the photocatalytic H₂-production activity of P2 to some extent.

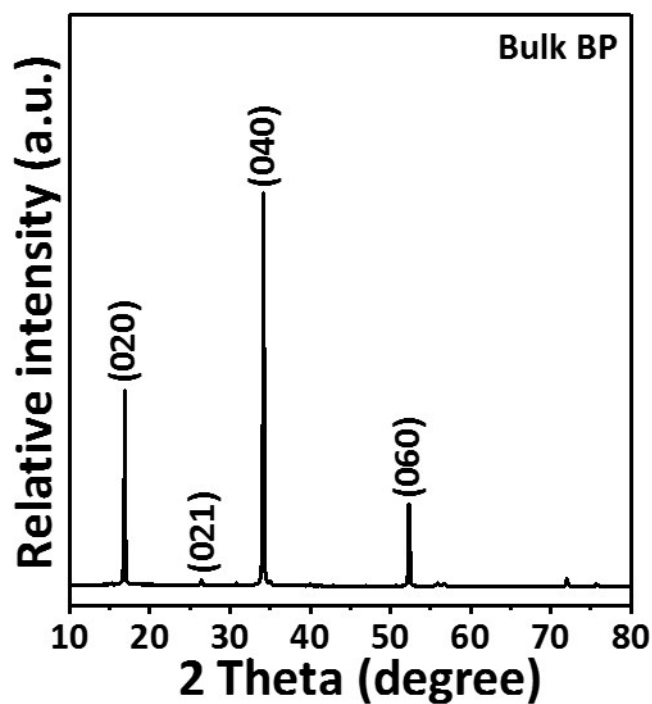


Fig. S5. XRD pattern of bulk BP.

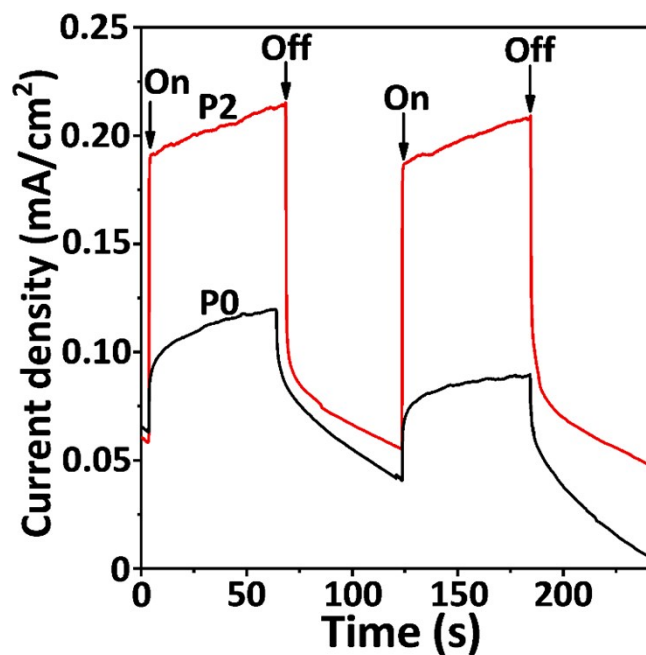


Fig. S6. Transient photocurrent response of P0 and P2 electrodes in 0.2 M Na₂S and 0.04 M Na₂SO₃ aqueous solution under visible-light illumination.

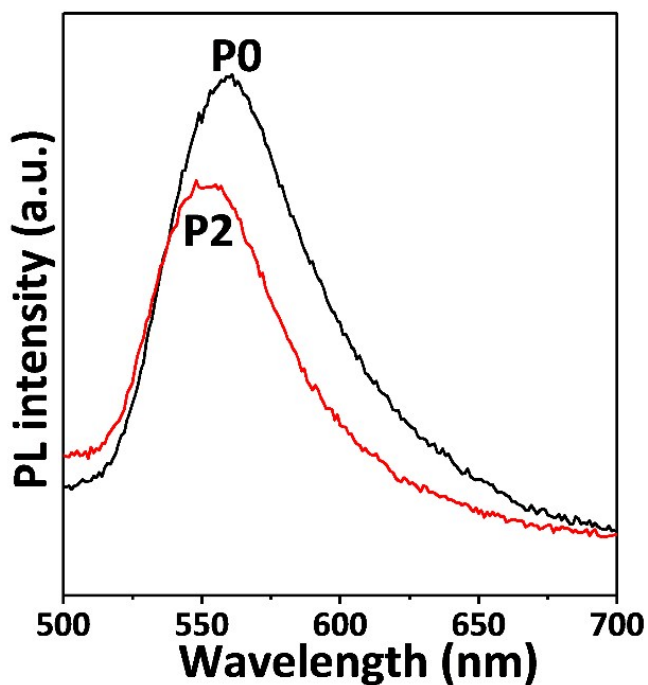


Fig. S7. Steady-state photoluminescence spectra of P0 and P2.

As shown in Fig. S7, the photoluminescence (PL) peak of P2 exhibits a clear blue shift compared to that of P0. This is due to the higher dispersion of ZCS NPs on the FLP NS in P2, resulting in smaller size and the stronger quantum confinement effect of ZCS NPs aggregation. Hence, the band gap of ZCS NPs aggregation in P2 is enlarged, thus leading to the blue shift of PL peak of P2.”

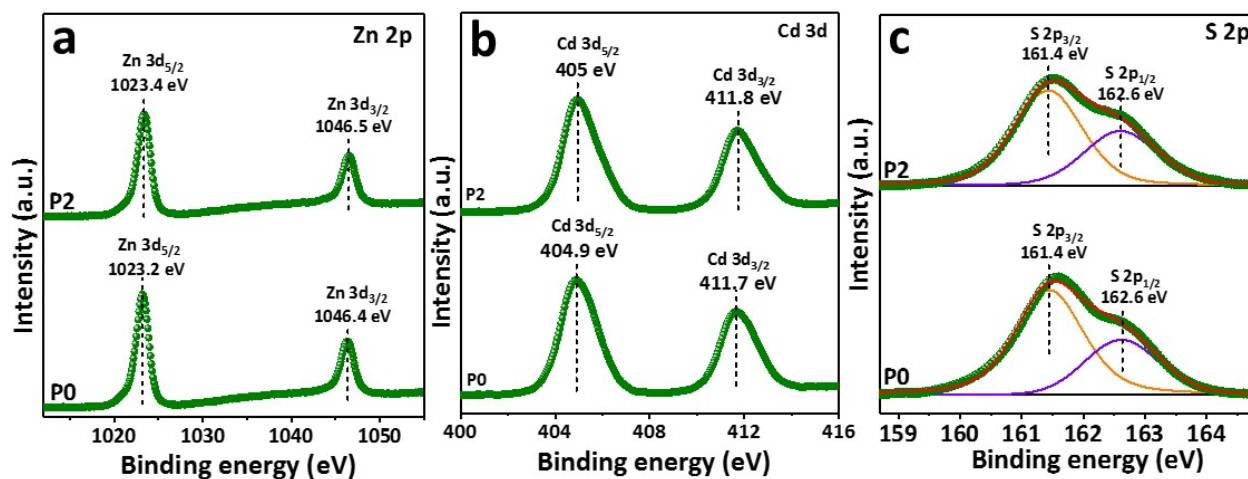


Fig. S8. High-resolution XPS spectra of (a) Zn 2p, (b) Cd 3d and (c) S 2p for P0 and P2.

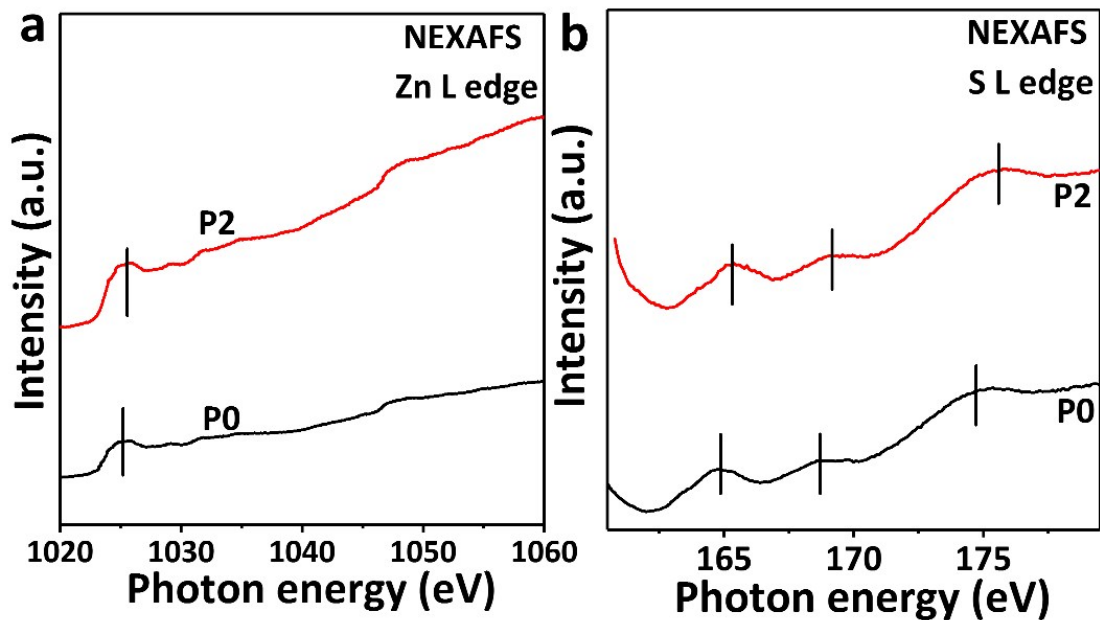


Fig. S9. (a) NEXAFS Zn L edge and (b) S L edge of P0 and P2.

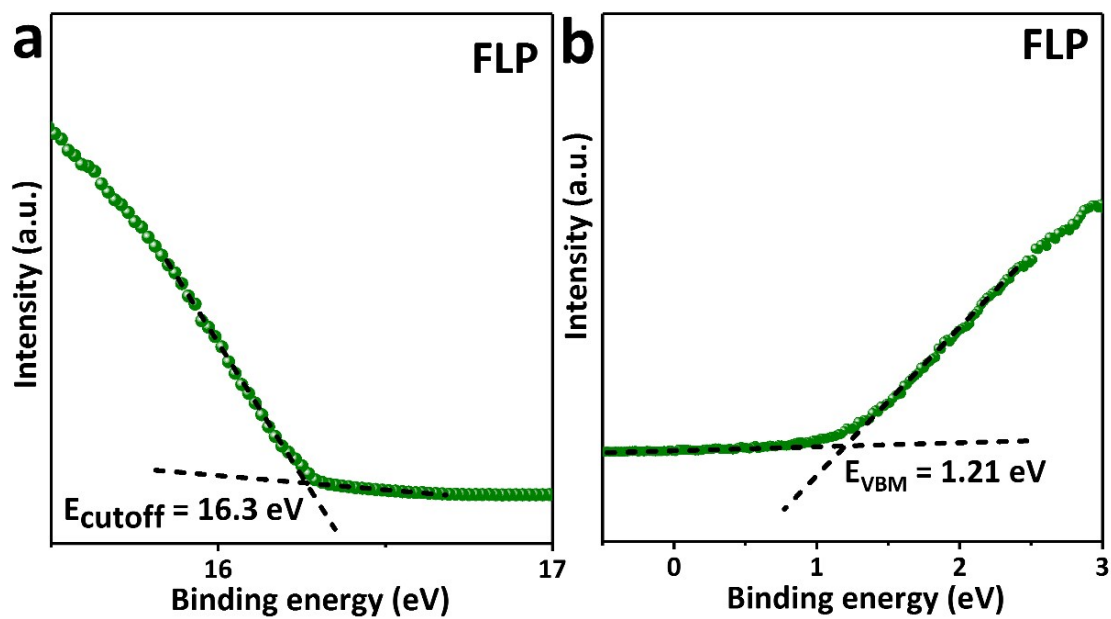


Fig. S10. UPS spectrum of (a) E_{cutoff} and (b) E_{VBM} for FLP.

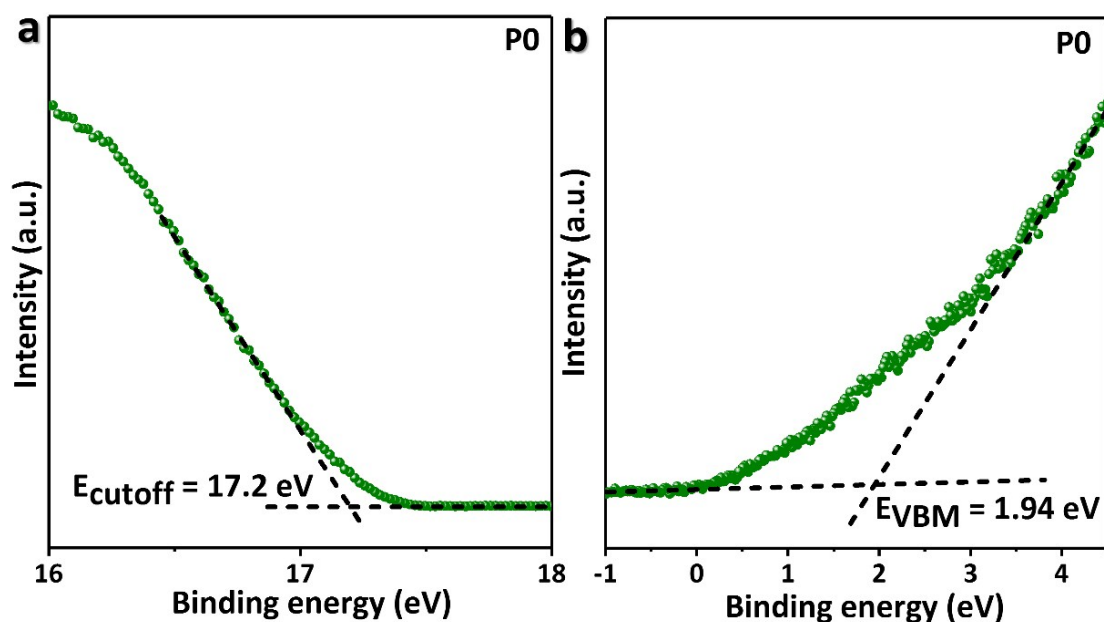


Fig. S11. UPS spectrum of (a) E_{cutoff} and (b) E_{VBM} for P0.

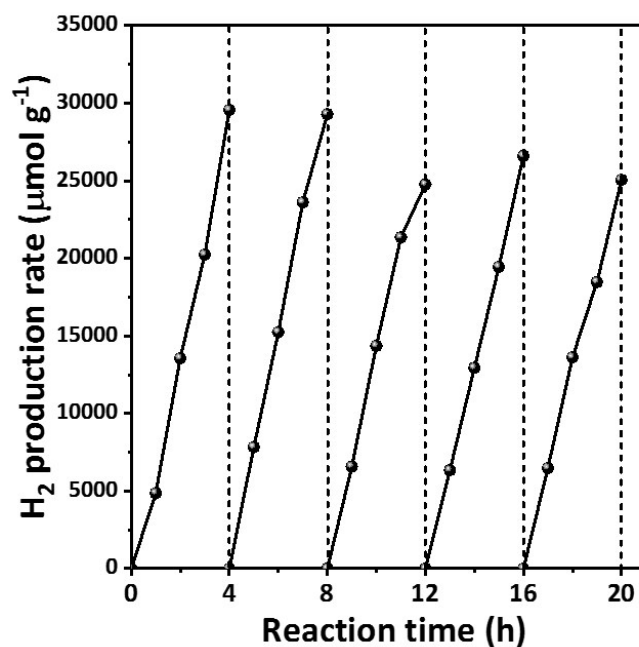


Fig. S12. Time course of photocatalytic H_2 production over P2 ($\lambda \geq 420 \text{ nm}$, 300 W Xe lamp); the reaction system was bubbled with Ar for 30 min to remove H_2 every 4 hours.

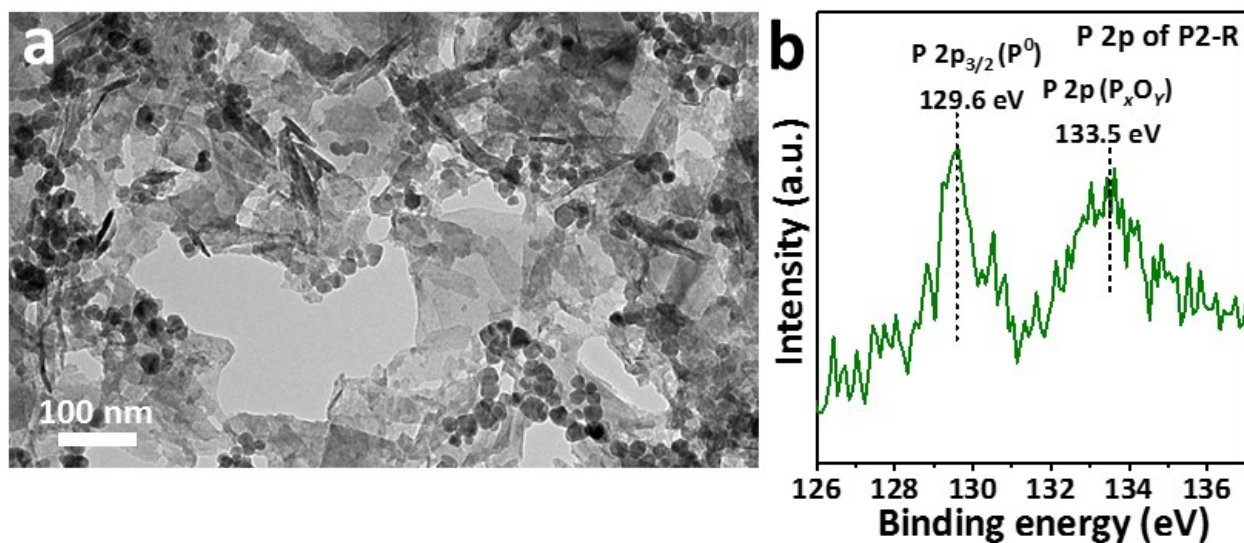


Fig. S13. (a) TEM image and (b) high-resolution XPS spectrum of P 2p for P2-R.

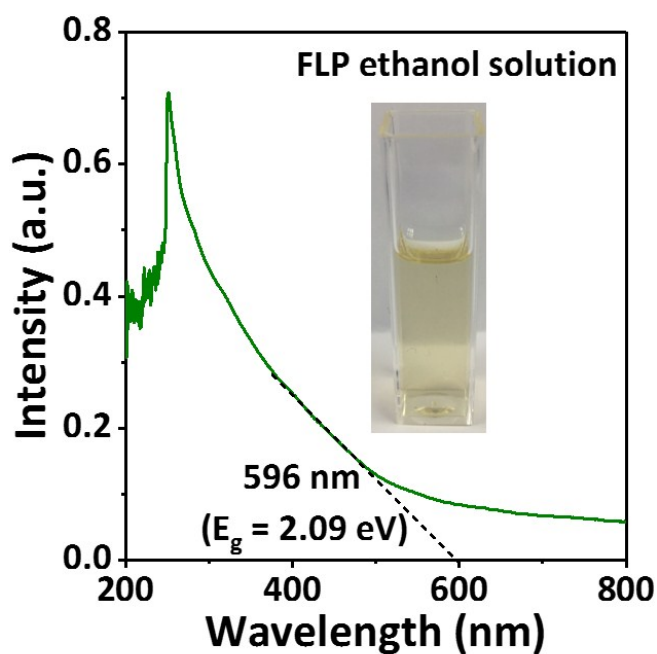


Fig. S14. UV-Vis absorbance spectra of FPS in ethanol solution. The inset shows the picture of FPS dispersed in ethanol solution.

Table S1. Physico-chemical properties of P0 and P2.

Samples	P (wt.%) (ICP-AES)	S_{BET} ($\text{m}^2 \text{g}^{-1}$)	PV ^a ($\text{cm}^3 \text{g}^{-1}$)	APS ^b (nm)	ACS ^c (nm)	H ₂ production rate ($\mu\text{mol h}^{-1} \text{g}^{-1}$)
P0	0	48.6	0.24	19.7	12.0	484
P2	1.78	42.1	0.24	23.1	12.0	9326

^a PV: Pore volume, ^b APS: Average pore size, ^c ACS: Average crystallite size (002).
